

International Conference On Medical Imaging Understanding and Analysis 2016, MIUA 2016,  
6-8 July 2016, Loughborough, UK

## An integrated software application for non-invasive assessment of local aortic haemodynamic parameters

Mateusz Florkow<sup>a,b</sup>, Jorge Mariscal Harana<sup>a</sup>, Arna van Engelen<sup>a,\*</sup>, Torben Schneider<sup>c</sup>,  
Isma Rafiq<sup>a</sup>, Hubrecht de Blied<sup>d</sup>, Jordi Alastruey<sup>a</sup>, Rene Botnar<sup>a</sup>

<sup>a</sup>*Division of Imaging Sciences and Biomedical Engineering, St. Thomas' Hospital, King's College London, London, UK*

<sup>b</sup>*Philips Research, Cambridge, UK*

<sup>c</sup>*Philips Healthcare, Guildford, Surrey, UK*

<sup>d</sup>*Philips Healthcare, Best, Netherlands*

---

### Abstract

Non-invasive assessment of haemodynamic data, such as pressure and flow profiles, is helpful in detecting cardiac disease at an early stage. However, current methods lack spatial accuracy and do not take local variations into account. This paper presents a software tool that extracts the arterial geometry and blood inflow profiles from MR images, which are subsequently used to run a 1D haemodynamic simulation model, and displays its output. The workflow is highly automated but allows user-interaction to correct inaccuracies. The tool was evaluated for inter-observer agreement on one healthy volunteer, and results are shown for one patient with an aortic coarctation. The resulting haemodynamic parameters show high agreement between different users and reveal local changes within a coarctation patient.

© 2016 The Authors. Published by Elsevier B.V.

Peer-review under responsibility of the Organizing Committee of MIUA 2016.

### Keywords:

Cardiovascular disease; MRI; haemodynamics; platform software

---

## 1. Introduction

Cardiovascular diseases are one of the leading causes of death worldwide, accounting for almost 33% of global deaths in 2013<sup>4</sup>. Early detection of changes in cardiovascular function is important to allow timely intervention and to restore or maintain cardiovascular health. Some physiological quantities such as blood pressure (BP) may be affected long before anatomic changes, such as luminal expansion, become apparent and hence are promising early biomarkers for cardiovascular disease detection. Traditionally, BP and blood flow are measured non-invasively. For example, BP is typically measured via a cuff placed at the brachial artery. However, these measurements provide global or peripheral data, instead of local anatomy-specific parameters which may be of interest to assess local variation in the vessel's

---

\* Corresponding author

E-mail address: [arna.van.engelen@kcl.ac.uk](mailto:arna.van.engelen@kcl.ac.uk)

properties. Currently, localised haemodynamic parameters can only be obtained via highly invasive procedures, such as invasive catheter measurements. An alternative approach to non-invasively obtain localised haemodynamic parameters is the use of computational modelling. MRI-derived quantities such as 3D arterial geometry and inflow profiles of an arterial segment can be used as inputs for such models to provide local estimates of flow, velocity and pressure waveforms along the artery of interest. The purpose of this work is to present an integrated software package to quantify and visualise local pressure, flow and velocity along an artery, combining MR image analysis and 1D haemodynamic modelling. We will demonstrate the workflow on a typical MRI dataset of the aorta of a healthy volunteer and a patient with aortic coarctation. Furthermore we will assess the inter-observer reproducibility of our semi-automatic aortic segmentation and its impact on the generated modelling output.

## 2. Methodology

An overview of the entire workflow is provided in figure 1. The input parameters for the 1D haemodynamic model, which computes local haemodynamic parameters, are derived from MR datasets (flow and 3D anatomy). The remainder of this section explains each of the processing steps in detail, followed by a description of the experimental set-up used to evaluate the proposed framework. All steps required for MR image analysis, manual interaction and visualisation of results have been integrated in one software tool implemented in C#. The computational modelling algorithm was implemented in C and is currently interfaced from the software tool via disk files.

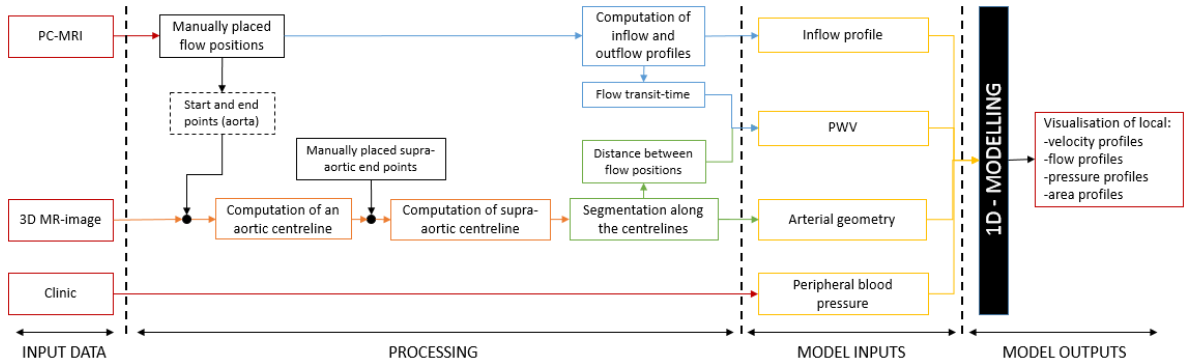


Fig. 1. Processing pipeline. Five points are placed on MR images to be the start or end points of vessels' centrelines. Two (in the aorta) are placed on phase contrast (PC) MR images to obtain blood flow profiles and to compute the aortic centreline, the other three define end points of supra-aortic arteries. Junction points are defined between the aorta and its side branches and, along all centrelines, a segmentation is performed to obtain the arterial geometry. This geometry, the inflow profile, pulse wave velocity (PWV) and peripheral blood pressure are provided to the 1D modelling and its output parameters are obtained and visualised.

### 2.1. Arterial geometry and segmentation

The segmentation of the aorta and the three supra-aortic arteries is performed on 3D MRI data and can be subdivided into three steps. First, a centreline is tracked within the aorta and its lumen is segmented every centimetre to obtain cross-sectional area. Subsequently, for each supra-aortic artery, the centreline and lumen area are calculated in a similar fashion.

#### 2.1.1. Centreline tracking

Centreline tracking is performed automatically between two predefined points. In our workflow, for the abdominal and descending aorta, the start and end points are defined based on the position of the inflow and outflow measurement (see 2.2), whereas for the supra-aortic arteries, one manually-defined end point within the artery is required (see 2.1.3).

The centreline algorithm follows three steps. First a vesselness filter, based on the filter of Frangi et al.<sup>2</sup> is performed to enable tube detection using the eigenvalues of the Hessian matrix. Then, a bi-directional fast marching algorithm is applied from both start and end points as described by Wink et al.<sup>5</sup> to find the minimal path. The last step is to centre and smooth the centreline using an active contour.

The performance and success of the algorithm is dependent on the quality of the input image data. For improved accuracy, manual correction of the centreline is possible.

### 2.1.2. Lumen segmentation

The centreline is resampled at equidistant locations that will define the input locations for the haemodynamic model. At these locations, a segmentation based on Wink et al.<sup>6</sup> is performed: rays are cast outward from the seed and the border of the vessel is found at the maximum image gradient. This is performed in a plane perpendicular to the vessel axis, defined using the previous and next points on the centreline. In the end, the segmented lumen is defined as a series of rings.

### 2.1.3. Merging of centrelines

To merge the supra-aortic centrelines with the main aortic centreline, a supra-aortic centreline is computed between the supra-aortic endpoint and the start point of the main aorta. The distance between the two centrelines is then calculated at each control point. When the distance becomes smaller than a third of the average radius of the aorta, the control point on the aortic centreline is set as the junction point. This junction point is then used as the new start point to compute the final supra-aortic artery centreline.

Once the segmentation along the centrelines is computed, some rings in the supra-aortic arteries will be located within the main aortic geometry as shown in figure 2 (a). This is problematic since the haemodynamic model does not allow duplication between the volumes of the different arteries to produce accurate results. To address this problem, all rings on the side branch whose distance to the junction point is less than the average radius of the aorta are automatically removed. To ensure that the two branches are completely separated, the user can remove additional rings manually. Hence, the first ring of the supra-aortic artery does only belong to the supra-aortic artery and not to the aorta. Once this is the case, some rings of the main aorta that extend into the side branches (figure 2 (b)) may need to be edited. All control points of these rings that are above the aforementioned first ring of the side branch are removed automatically, resulting in a clipped aortic segmentation such that no volume is duplicated for the modelling.

### 2.1.4. Managing inaccurate segmentation

Even after the semi-automatic corrections described above, in some cases the vessel segmentation can still be inaccurate due to variation in the intensity of the voxels in the lumen or poor intensity gradients at the wall. Therefore, an additional post-processing step allows the user to remove rings by setting a user-defined minimum and maximum area per centreline to remove these outliers. Furthermore, single segmentations can be removed manually to improve the segmentation.

## 2.2. Flow MRI analysis

Volumetric blood flow profiles at the start and end of the main aortic centreline are required as input parameters to the model and to derive a global pulse wave velocity (PWV) which is another input parameter. These profiles are extracted from time-resolved 2D phase contrast (PC) MR images from which the through-plane velocity can be quantified. Given a manually-placed seed at a single time frame, delineation of the inner wall of the vessel is achieved

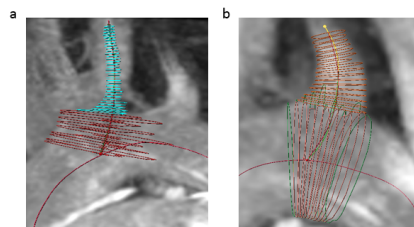


Fig. 2. (a) Rings calculated on a supra-aortic artery. In red, rings that will be removed as they are in the aorta; (b) In green, rings as computed in the aorta by the segmentation algorithm. In pink, optimised rings in the aorta to separate the vessel from supra-aortic arteries. In orange, rings in a supra-aortic artery. For demonstration purposes, rings are computed every millimetre.

via aforementioned automatic segmentation in the 2D image plane. The segmentation is then propagated throughout the entire cardiac cycle based on similar image gradients to obtain the vascular cross sectional area at all phases. Time-resolved flow profiles are obtained by integrating velocity over the luminal area for each time frame.

To calculate PWV of the full aortic segment, a foot-to-foot method<sup>3</sup> is used. The feet of the flow profiles are defined as the intersection between the tangent at the inflexion point of early systole and a horizontal line passing through the local minimum. The difference of the feet x-coordinate between the inflow and outflow profiles is the transit time. The length of the arterial segment is determined from the previously calculated centreline, and is divided by transit time to obtain PWV.

### 2.3. Haemodynamic model

Once the arterial geometry, PWV and in-vivo pressure are known, the 1-D model parameters are calculated. For computational purposes, the arterial geometry is represented as a set of nodes connected with 1-D model segments. Each segment has an inlet and an outlet. This geometric information is stored in an  $N$  by  $S$  matrix, where  $N$  and  $S$  are the number of nodes and segments, respectively. At bifurcations between the aorta and any supra-aortic vessel, the two daughter segments share the same inlet node.

At the inlet of the ascending aorta, a periodic inflow boundary condition, measured in-vivo using phase-contrast MRI, is prescribed. Three-element Windkessel models are used as outflow boundary conditions at the outlets of the descending aorta and the supra-aortic vessels. The outflow at the aorta is measured from PC-MRI and the distribution of outflow at each supra-aortic artery is estimated based on vessel cross-sectional area. For these outflow models, nonlinearities and inertia effects are neglected.

Vessel lengths and areas from MRI segmentation, together with material properties and inflow boundary conditions obtained in-vivo, allow us to simulate 1-D blood flow within the aorta and supra-aortic vessels. The haemodynamic simulation software, Nektar1D, uses a finite element scheme in order to solve the nonlinear, 1-D equations of blood flow within compliant vessels. The resulting simulations yield velocity, area and pressure curves at any location along the main aortic and supra-aortic centrelines. Further details on the 1D formulation and its numerical solution are given by Alastruey et al.<sup>1</sup>.

### 2.4. Experiments

We evaluated the proposed workflow in a healthy 30-year-old male and a 28-year-old patient post-coarctation repair. Two 2D-PC flow datasets were acquired (125 reconstructed phases, field of view (FOV): 280/350mm, echo time (TE): 2/3ms, repetition time (TR): 4/5ms, field strength (FS): 1.5T) at the start of the ascending aorta and in the descending thoracic aorta. For the healthy volunteer a 3D steady-state free precession MR image (FOV: 320mm, TE: 3ms, TR: 5ms, FS: 1.5T) was used to obtain the geometry, and for the patient a 3D contrast-enhanced MRA dataset (FOV: 500mm, TE: 1ms, TR: 5ms, FS: 1.5T, 31s post contrast-administration) was used.

All steps, as described in figure 3 and in the previous sections, were followed. To evaluate the stability of the procedure, three different users, members of the development team, each performed the entire workflow for the healthy volunteer, including all manual interactions on the centreline and segmented arteries they deemed necessary. Output profiles for flow, pressure, velocity and area were obtained for each segment of the main aortic centreline.

## 3. Results

A screenshot of the software is presented in figure 4. To guide the user through the different steps of the procedure, the user interface is organised with tabs. For a better perception of results, various kinds of display (3D models, graphs, tables) are used and adapted to the different inputs and outputs.

The segmentation result of one observer for the healthy volunteer is presented figure 5 (a). Local flow, pressure and velocity profiles were obtained in each segment along the aorta. To visualise variations in vessel area, the centreline is color-coded as illustrated figure 5 (a).

Flow, pressure and velocity profiles can be displayed for each segment. A comparison between the flow and pressure profiles obtained by the three different users at the junction between the aorta and the carotid artery is

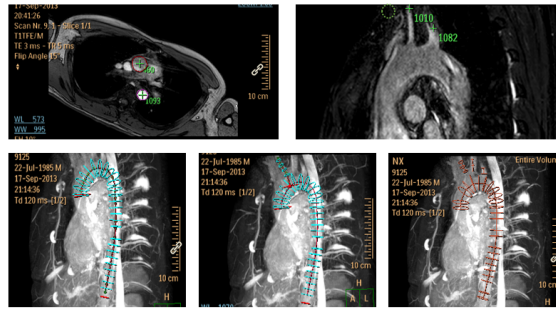


Fig. 3. (a) First, a seed is placed on 2D PC-MR images to indicate the flow location and serves as start (if ascending aorta) or end (if descending aorta) point for the aortic centreline; (b) Then, multiplanar reconstruction is used to place one end point for each supra-aortic centreline; (c) With those five user-defined points, aorta is first delineated (left) before its connection with each side branch (middle) to obtain a fully segmented aorta with its three supra-aortic arteries (right).



Fig. 4. Screenshot of the software. The left pane shows the tabs for the different steps to guide the user. The right pane shows on top from left to right the two PC MRI images with the aorta segmented, a color-coded centreline displaying area, the segmented artery, and on the bottom row the MR image used to define supra-aortic end points, input flow curves and table with results.

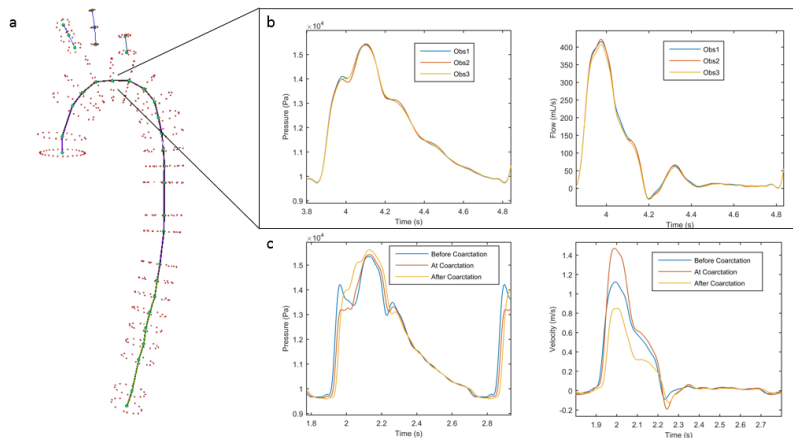


Fig. 5. (a) Result of a segmentation: nodes (green spheres) are connected with area color-coded segments. The colormap goes from blue (high values) to yellow (low values). At each node, the artery was segmented (red ring); (b) Comparison between the flow and pressure waveforms obtained by the three users at the junction of the aorta and the carotid; (c) Comparison between the flow and pressure waveforms of a coarctation patient before, at and after the narrowing.

shown in figure 5 (b). The obtained flow, pressure and velocity profiles are highly reproducible between observers as

Table 1. Relevant parameters obtained by the three observers at the junction between the carotid and the aorta (Junction) and in the descending aorta (DAo).

Observers	Stroke volume (mL)		Max. flow (mL/s)		Max. pressure (kPa)		Max. velocity (m/s)	
	Junction	DAo	Junction	DAo	Junction	DAo	Junction	DAo
Obs 1	81.1	67.3	415	258	15.40	15.95	0.66	0.67
Obs 2	80.3	67.3	422	283	15.44	15.84	0.64	0.72
Obs 3	77.2	67.2	407	255	15.38	15.79	0.62	0.78

described table 1. Figure 5(c) presents the results in a patient with coarctation in the descending aorta, before, at and after the narrowing. Flow velocity increases at the coarctation, which is coherent with a decrease of the aortic radius.

#### 4. Discussion and Conclusion

We presented a platform that semi-automatically extracts arterial geometry and PWV from MR images and displays local haemodynamic parameters obtained through 1D modelling. We designed the software to be user-friendly such that it can easily be integrated in a clinical research workflow. The obtained results are robust and localised. Our software provides a straightforward way to non-invasively study local haemodynamic parameters in different populations.

The development of the software and the implementation of the 1D model are still works-in-progress. We are working on improvements of visualisation and manual editing capabilities of the lumen segmentation, which would help to further increase the accuracy of vessel geometry data, especially in low quality images. On the modelling side, we will investigate the use of outflow profiles of the supra-aortic arteries. This would lead to more accurate results, but in practice this data is often not present. Secondly, to improve the modelling results, it may be advantageous to include a way to account for energy losses that usually occur at vessel narrowing. This would allow for more accurate results in conditions such as coarctation where pressure drops are expected. In the future, we will also fully integrate the 1D modelling into the software platform to overcome the need to export and import data for use in a different tool. Furthermore, we aim to perform a more elaborate analysis of the results obtained using this software, by including more datasets and different diseases and vessels, and possibly compare our results with manually segmented arteries.

To conclude, the platform provides image processing tools that can be used to easily obtain and visualise multiple cardiovascular parameters derived from various MR datasets and patients. The highly automated workflow still allows user-interaction and gives robust and promising results. Our integrated software is an important step towards enabling large scale applications of haemodynamic modelling in clinical research.

#### 5. Acknowledgements

This research has been supported by an EPSRC Technology Strategy Board CR&D Grant (EP/L505304/1) and an EPSRC Grant EP/K031546/1.

#### References

1. Jordi Alastruey, Kim H. Parker, and Spencer J. Sherwin. Arterial pulse wave haemodynamics. In *11th International Conference on Pressure Surges*, pages 401–442. Virtual PiE Led t/a BHR Group: Lisbon, Portugal, 2012.
2. Alejandro F. Frangi, Wiro J. Niessen, Koen L. Vincken, and Max A. Viergever. Multiscale vessel enhancement filtering. In *Medical Image Computing and Computer-Assisted Intervention MICCAI98*, pages 130–137. Springer, 1998.
3. NR Gaddum, J Alastruey, P Beerbaum, P Chowienczyk, and T Schaeffter. A technical assessment of pulse wave velocity algorithms applied to non-invasive arterial waveforms. *Annals of biomedical engineering*, 41(12):2617–2629, 2013.
4. GBD 2013 Mortality and Causes of Death Collaborators. Global, regional, and national agesex specific all-cause and cause-specific mortality for 240 causes of death, 1990–2013: a systematic analysis for the Global Burden of Disease Study 2013. 385(9963):p117–171, January 2015.
5. O Wink. *Vessel Axis Determination for Diagnosis and Treatment*. PhD thesis, 2004.
6. Onno Wink, Wiro J. Niessen, and Max A. Viergever. Fast delineation and visualization of vessels in 3-D angiographic images. *Medical Imaging, IEEE Transactions on*, 19(4):337–346, 2000.